

## DEFORMATION OF LIQUID MENISCI UNDER THE ACTION OF AN ELECTRIC FIELD

G. JOFFRE, B. PRUNET-FOCH, S. BERTHOMME and M. CLOUPEAU

*Laboratoire d'Aérothermique du CNRS, 4ter, route des Gardes, 92190 Meudon (France)*

(Received November 30, 1981; accepted in revised form April 5, 1982)

### Summary

A calculation method is proposed for the determination of profiles of stable menisci formed at one end of a capillary raised to an electric potential. No simplifying hypothesis has been made with respect to the form of the meniscus and the configuration of the electric field to solve simultaneously the Laplace equation relative to potential and the pressure balance equation at the liquid surface. The profiles and maximum heights of the stable menisci determined experimentally show good agreement with theoretical results.

---

### Notation

$A$	surface tension of liquid
$D$	capillary end/plate distance
$E_s$	electric field at the surface of the meniscus
$g$	acceleration due to gravity
$H$	height of liquid in relation to capillary outlet plane
$K_1, K_2$	constants: $K_1 = \rho g R^2/A$ , $K_2 = H/R$
$p_c$	capillary pressure
$p_h, p_h^0$	hydrostatic pressure, at a point of the meniscus surface and at the capillary orifice
$r$	radial distance from a point to the capillary axis
$R$	radius of capillary orifice
$R_1, R_2$	principal radii of curvature at each point of the meniscus surface
$U$	potential at each point of the domain
$U_0$	potential on the capillary and the meniscus
$z$	ordinate of a point from the capillary outlet plane
$z_s$	ordinate of a point on the meniscus surface in relation to the capillary outlet plane
$z_M$	height of meniscus on axis
$\epsilon_0$	dielectric constant of the medium

$\rho$  liquid density  
 $\sigma$  surface charge density

Sub- and superscripts:

( $\bar{\quad}$ ) dimensionless quantity  
 s liquid surface

## 1. Introduction

If a capillary tube is fed with liquid at a relative pressure approaching zero, and is raised to an increasing electric potential, the height of the meniscus formed at the free end of the capillary tube increases progressively. At a sufficiently high potential, the electrostatic pressure at the surface becomes high enough for the meniscus to become unstable, leading to the emission of charged droplets. This system can produce particles varying widely in size, ranging from 1 mm to a few tens of angströms. Depending on the experimental conditions, it operates in dropping mode [1], produces fine aerosols [2–5], and can even constitute an ion emitter [6]. Several operating modes have been described since 1915 by Zeleny [7], and electrohydrodynamic spraying (EHD) has attracted many investigators since then [8].

During fine spraying, the meniscus often displays the form of a cone, the base of which is the outlet cross-section of the capillary tube, and the apex may be prolonged by a thin liquid filament. Droplets are produced by breakage of the filament, or are emitted at the apex of the cone [8].

To understand the droplet formation mechanism, it is necessary to be able to calculate the form of the menisci. As a rule, this requires the simultaneous solution of the pressure balance equation at each point of the liquid surface and the Laplace equation relative to potential. To simplify this complex problem, several workers have assumed the form of the meniscus [9,10] or the distribution of the electric charge [1]. These assumptions served to obtain interesting results but were valid only for specific conditions.

In order to have a computation method for which the field of application is less restricted, we decided to develop a numerical method that serves to solve simultaneously the equations expressing the pressure balance and the potential distribution. The first results that are discussed in this article are concerned only with stable menisci of rounded shape, which do not give rise to the emission of droplets or electric charges. With the profiles of menisci obtained for different parameter values, and the corresponding menisci heights, the computations yield critical potentials above which the menisci become unstable and change suddenly to other forms (which may or may not be stable).

## 2. Previous works and general equations

Profiles of pendent or sessile drops and liquid bridges have formed the sub-

ject of many investigations [11–16]. Most of these studies were aimed to improve methods for measuring liquid surface tensions.

In the absence of any electric field, the profile of stable menisci appearing at the end of a vertical tube can be determined by solving the equation that reflects the hydrostatic and capillary pressure balance at each point of the meniscus surface.

By taking the end of the capillary tube as a reference level, the hydrostatic pressure  $p_h$  at a point on the meniscus surface with ordinate  $z_s$  (Fig. 1) can be written ( $z_s$  is counted positively downwards, and  $H$  is counted positively upwards):

$$p_h = \rho g (z_s + H) \quad (1)$$

where  $\rho$  is the liquid density and  $g$  the acceleration due to gravity.

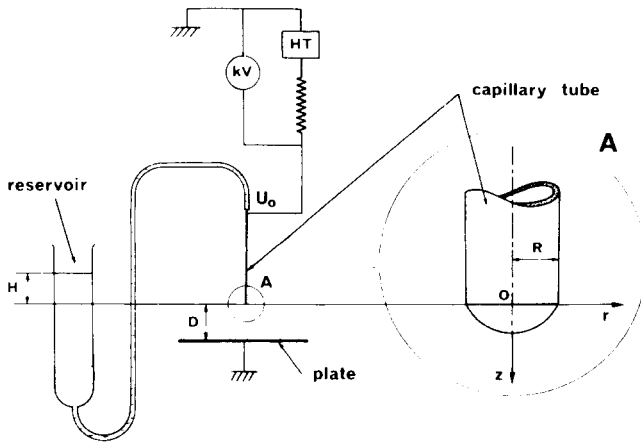


Fig. 1. Experimental assembly and definition of some symbols.

The term  $\rho g H$  represents the pressure  $p_h^0$  at the orifice of the tube. This is assumed to be produced by a column of the same liquid as the meniscus, and of height  $H$ .

The capillary pressure  $p_c$  is given by the Young/Laplace formula:

$$p_c = A \left( \frac{1}{R_1} + \frac{1}{R_2} \right) \quad (2)$$

where  $A$  is the liquid surface tension and  $R_1$ ,  $R_2$  the principal radii of curvature of the meniscus surface at the point considered.

The pressure balance leads to:

$$A \left( \frac{1}{R_1} + \frac{1}{R_2} \right) + \rho g (z_s + H) = 0 \quad (3)$$

In 1883, Bashforth and Adams [11] solved eqn. (3) in the case of pendent and sessile drops, using Taylor's series, and published tables giving the or-

ordinate  $z_s$  as a function of radial distance  $r$  for each point of a meniscus. In 1886, Lord Kelvin [12] obtained profiles of sessile drops by geometric construction. This method was repeated by Cross and Picknett [13] in 1963. The tables of Bashforth and Adams were supplemented by several authors. All the results were gathered together in 1969 by Padday [14], who himself calculated profiles of drops and liquid bridges of many types [15]. Finally, in 1974, Kovitz [16] showed that for a given value of the hydrostatic pressure two solutions are available for eqn. (3), the first representing a stable equilibrium and the second a metastable equilibrium.

If the liquid surface is raised to a high potential in relation to a nearby plate, the electrostatic pressure exerted by the surface charges changes the profile of the surface. This electrostatic pressure is proportional to the square of the surface charge density  $\sigma$ , and inversely proportional to the dielectric constant  $\epsilon_0$  of the medium. In these conditions, the balance equation becomes:

$$A \left( \frac{1}{R_1} + \frac{1}{R_2} \right) + \rho g(z_s + H) + \frac{\sigma^2}{2\epsilon_0} = 0 \quad (5)$$

This equation can only be solved if the density  $\sigma$  is known, and this density can only be calculated from the solution of the Laplace equation relative to the potential  $U$ :

$$\Delta U = 0 \quad (5)$$

Hence it is necessary to solve simultaneously eqns. (4) and (5); this raises various difficulties. This matter has only been dealt with hitherto in specific cases or by introducing simplifying hypotheses.

Thus Taylor [9] theoretically confirmed the possibility of the existence of cones with a straight generating line. For such a meniscus geometry, the capillary pressure at each point varies inversely with the distance from the tip of the cone. By looking for a solution to the Laplace equation such that the absolute value of the electrostatic pressure is equal at each point on the surface to that of the capillary pressure, Taylor found that equilibrium can be achieved if the half-angle at the apex of the cone is equal to  $49.3^\circ$ . This form has effectively been observed, at least as a transient state, just before the initiation of the spraying mechanism. However, the validity of this theoretical result, obtained by imposing the shape of the meniscus, is also limited to a clearly defined geometry of the support and to the case of zero hydrostatic pressure. Moreover, the method employed does not indicate positively whether the cone is a stable form.

In 1978, Borzabadi and Bailey [1] investigated the profile of pendent drops raised to a given potential in relation to a plane plate perpendicular to the capillary axis. These workers avoided solving the Laplace equation by assuming that the charge density at the periphery of a cross-section of diameter  $d$  is equal to the density calculated by the formula of Van Dyke [17] for a semi-infinite cylinder of the same diameter  $d$ . As this calculation

leads to an infinite field at the tip of the drop, they compare the surface in the vicinity of this extremity to a paraboloid and apply Becker's [18] expression for the field to this region. A comparison of theoretical and experimental results shows that these approximations are only acceptable if the profiles obtained are fairly elongated in shape.

To calculate the shape of electrified menisci, we attempted to solve, without simplifying assumptions, the system of eqns. (4) and (5) by a numerical method that serves to deal with the case of stable menisci in which the hydrostatic, capillary and electrostatic pressures are balanced.

### 3. System of equations serving to determine the form of menisci

#### 3.1. Dimensionless equations

The equilibrium condition of the meniscus formed at the end of a capillary tube raised to potential  $U_0$  in relation to a plate (Fig. 1) is given by eqn. (4) which can be written in dimensionless form:

$$K_1(K_2 + \bar{z}_s) + \left( \frac{1}{\bar{R}_1} + \frac{1}{\bar{R}_2} \right) + \frac{\bar{\sigma}^2}{2} = 0 \quad (6)$$

where  $K_1$  and  $K_2$  are the dimensionless groups defined by:

$$K_1 = \rho g R^2/A \text{ and } K_2 = H/R$$

and where  $\bar{z}_s$ ,  $\bar{R}_1$ ,  $\bar{R}_2$  and  $\bar{\sigma}$  are dimensionless variables defined by:

$$\bar{z}_s = z_s/R \text{ ,}$$

$$\bar{R}_1 = R_1/R$$

$$\bar{R}_2 = R_2/R$$

$$\text{and } \bar{\sigma} = \frac{\sigma}{\sqrt{\epsilon_0 A/R}} \text{ .}$$

In the case of symmetry of revolution, the term  $(1/\bar{R}_1 + 1/\bar{R}_2)$  is expressed as a function of derivatives of  $\bar{z}_s$  in relation to the radial coordinate  $\bar{r} = r/R$  by the equation:

$$\frac{1}{\bar{R}_1} + \frac{1}{\bar{R}_2} = \frac{\frac{\partial^2 \bar{z}_s}{\partial \bar{r}^2} + \frac{1}{\bar{r}} \frac{\partial \bar{z}_s}{\partial \bar{r}} \left[ 1 + \left( \frac{\partial \bar{z}_s}{\partial \bar{r}} \right)^2 \right]}{\left[ 1 + \left( \frac{\partial \bar{z}_s}{\partial \bar{r}} \right)^2 \right]^{3/2}} \quad (7)$$

Equation (6) then becomes:

$$K_1(K_2 + \bar{z}_s) + \frac{\frac{\partial^2 \bar{z}_s}{\partial \bar{r}^2} + \frac{1}{\bar{r}} \frac{\partial \bar{z}_s}{\partial \bar{r}} \left[ 1 + \left( \frac{\partial \bar{z}_s}{\partial \bar{r}} \right)^2 \right]}{\left[ 1 + \left( \frac{\partial \bar{z}_s}{\partial \bar{r}} \right)^2 \right]^{3/2}} + \frac{\bar{\sigma}^2}{2} = 0 \quad (8)$$

The differential equation in  $\bar{z}_s$  thus obtained can be solved if the value of the function  $\bar{\sigma}$  is known at each point. However, the surface charge density  $\sigma$  on a conductor is directly related to the field  $E_s$  at the surface by  $\sigma = \epsilon_0 E_s$ . In view of the dimensionless quantities defined above, this gives:

$$\bar{\sigma} = U_0 \sqrt{\epsilon_0 / AR} \bar{E}_s \quad (9)$$

where  $\bar{E}_s$ , the field modulus at the surface, is related to the potential gradient in the vicinity of the meniscus surface by the equation:

$$\bar{E}_s = \sqrt{\left(\frac{\partial \bar{U}}{\partial \bar{r}}\right)_s^2 + \left(\frac{\partial \bar{U}}{\partial \bar{z}}\right)_s^2} \quad (10)$$

where  $\bar{U} = U/U_0$ .

To obtain the value of  $\bar{\sigma}$  at each point, it is therefore necessary to determine the field  $\bar{E}_s$ ; this requires determination of the potential distribution in the neighbourhood of the liquid surface. This distribution can only be known by calculating the potential values in the entire space located between the liquid surface and the plate. Hence to solve eqn. (8), one must first solve eqn. (5).

The latter is written with dimensionless variables taking account of the symmetry of revolution:

$$\frac{\partial^2 \bar{U}}{\partial \bar{r}^2} + \frac{\partial^2 \bar{U}}{\partial \bar{z}^2} + \frac{1}{\bar{r}} \frac{\partial \bar{U}}{\partial \bar{r}} = 0 \quad (11)$$

### 3.2. Numerical analysis

Equations (8) and (11) were discretized to be solved numerically.

For eqn. (11), use was made of interpolation formulae in a non-uniform grid. The grid pitch, which is uniform and very small in the vicinity of the meniscus, increases by arithmetic progression with increasing distance from the meniscus, as shown in Fig. 2. The grid shown in this figure is of guidance value only. It does not give the exact number of meshes used, which is  $100 \times 40$  in reality.

Equation (11) was processed by a point-by-point over-relaxation method. The over-relaxation factor was calculated using formulae given by Girerd and Karplus [19]. The calculation was carried out column by column in the increasing  $r$  direction, with each column scanned from the meniscus to the plate.

Equation (8) was discretized using classic interpolation formulae in the same grid as above, and was solved using a step-by-step method (Newton's method).

### 3.3. Boundary conditions

In the case of a vertical semi-infinite capillary tube and an unlimited horizontal plate, the equipotentials at infinity are horizontal near the plate ( $\partial \bar{U} / \partial \bar{r} = 0$ ) and vertical near the capillary ( $\partial \bar{U} / \partial \bar{z} = 0$ ).

These conditions of the Newman type were imposed on the boundaries LM and MN of the computation domain (Fig. 2). It was confirmed that they

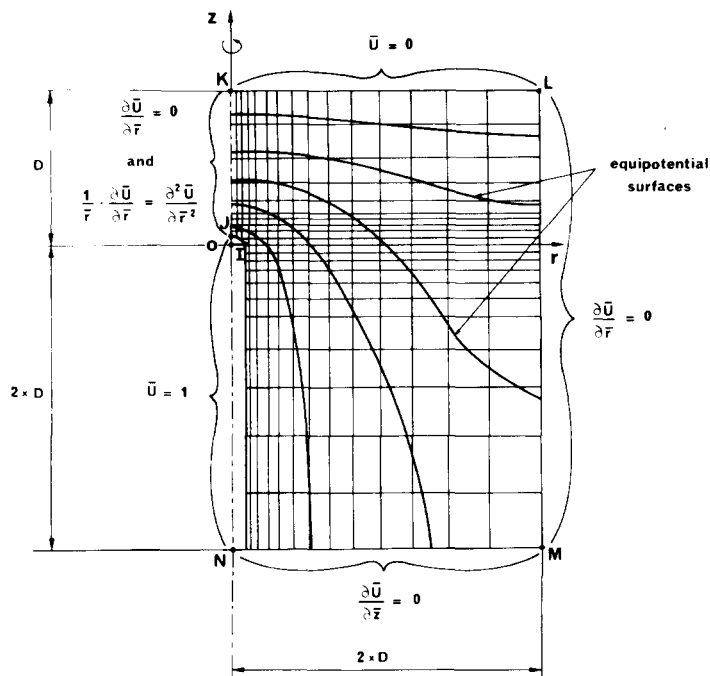


Fig. 2. Sketch of general grid.

had little effect on the equilibrium of the meniscus if the domain selected is sufficiently large:  $LM \geq 2D$ ,  $MN \geq 3D$ , where  $D$  represents the distance from the end of the capillary tube to the plate.

On axis  $Oz$ , the first derivatives of potential in relation to the radial coordinate  $r$  are nil in order to observe the symmetry of revolution. In addition, the product  $(1/r) (\partial \bar{U} / \partial r)$  keeps a finite value equal to the second derivative  $\partial^2 \bar{U} / \partial r^2$ .

On the meniscus and on the capillary, the boundary condition for the potential is of the Dirichlet type ( $\bar{U} = 1$ ); this also applies to the plate ( $\bar{U} = 0$ ).

### 3.4. Specific expressions in the vicinity of the meniscus

To obtain satisfactory accuracy in the vicinity of the meniscus in calculating the potentials (eqn. (11)) and the electric fields (eqn. (10)), it is necessary to consider the meniscus as an oblique boundary of the domain. Since the node to be used is below the meniscus (Fig. 3), it is replaced by the point located on the surface, making it necessary to use the formulae relative to a non-uniform grid again.

The boundary of the meniscus on the circular edge of the capillary forms a sharp edge at which a break occurs in the slope of the equipotential. In the vicinity of these singular points, the expressions used in the rest of the domain are not valid to calculate the potentials, and it is necessary to use

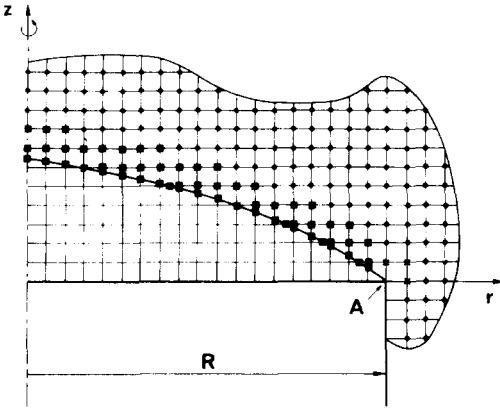


Fig. 3. Sketch of grid near meniscus: • nodes of the regular square grid; × nodes depending on the singular point A; ■ non-equidistant nodes.

special developments. These developments [20], which involve the use of Fourier series, are solutions to the Laplace equation. They account for the geometry of the conductor, especially the slope of the meniscus near the edge (Fig. 3).

### 3.5. Solution of equations

The equilibrium form of the meniscus for a given hydrostatic pressure  $p_h^0$  and potential  $U_0$  is obtained as follows.

An initial form of the meniscus is calculated with eqn. (8) for the hydrostatic pressure  $p_h^0$  and in the absence of an electric field. This form serves to calculate a potential distribution using eqn. (11) for the potential value  $U_0$ . In view of this distribution, eqn. (8) gives a new meniscus form. A new potential distribution is calculated, and so on.

At each stage, the solutions to eqns. (11) and (8) are considered satisfactory if the maximum difference between the values of two iterations is less than  $U_0/1000$  for the potentials and  $z_M/1000$  for the  $z_s$  ordinates of the meniscus surface.

The foregoing calculations are repeated until these convergence criteria are satisfied simultaneously for both equations.

This procedure is followed for increasing potentials  $U_0$  until the equations no longer provide equilibrium solutions. This corresponds to the case in which it is no longer possible to find a surface such that at each point the radii of curvature are sufficiently small for the capillary pressure to counterbalance the electrostatic pressure.

Hence, at a given hydrostatic pressure and for each value of  $U_0$ , the calculation gives the potential distribution in the entire space, that of the surface electric charge densities on the meniscus, and the profile of the meniscus. It also furnishes the maximum value of the capillary potential for which the meniscus remains stable.



No numerical instability was observed during the computations in the cases investigated.

The calculation method described applies to a vertical capillary that can be directed upwards as well as downwards. For the sake of convenience, most meniscus calculations were made on pendent drops, as experiments substantiating the results obtained are easier to perform in these conditions.

Figure 4 gives an example of the variations in a meniscus profile for different values of potential  $U_0$  at constant hydrostatic pressure  $p_h^0$ .

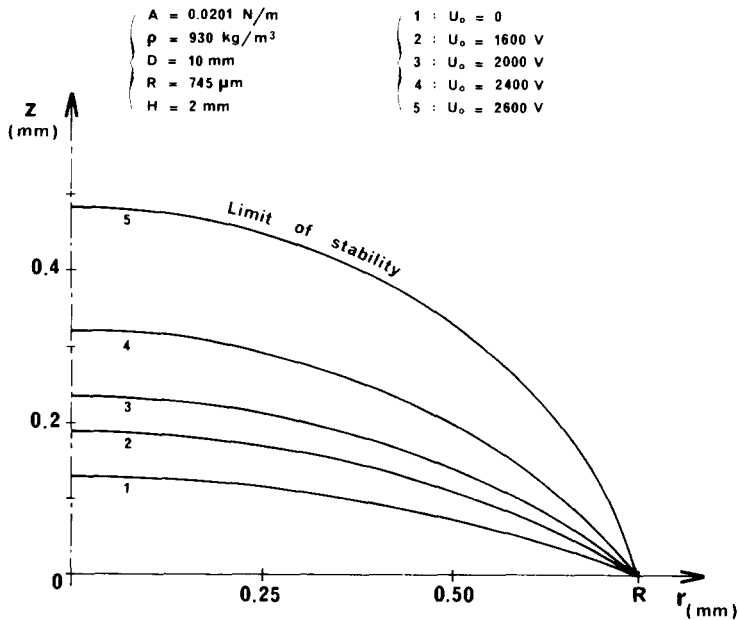


Fig. 4. Variation in profile of a meniscus for different values of potential  $U_0$  at constant hydrostatic pressure.

#### 4. Experimental

Experiments were conducted with the system shown schematically in Fig. 1. The capillary tubes were metal tubes with ends ground to obtain a circular cross-section with a sharp edge. They were 4 cm long and the outside diameters ranged from 460 to 1500  $\mu\text{m}$ . A high-voltage power supply was used to raise the capillary to a positive potential in relation to a plane plate connected to earth. This plate consisted of an 18 cm diameter disc placed at a distance  $D$  from the end of the capillary. In most of the experiments  $D$  was 10 mm.

To vary the hydrostatic pressure in the meniscus, the capillary was connected by a flexible tube to a reservoir of which the vertical position was adjustable. The height  $H$  of the liquid in the reservoir, in relation to the out-

let plane of the capillary tube, could be adjusted to within 1/100 mm, and the level for which the meniscus was flat was noted by means of a cathetometer.

The meniscus was observed or photographed at a magnification of 100 with a stereoscopic microscope with a free working distance of 10 cm, i.e. long enough for the microscope to avoid disturbing the electric field at the meniscus.

The comparison of theoretical and experimental results dealt with the height on the axis,  $z_M$ , which is a characteristic value of the meniscus, and in some cases with the entire profile. Several liquids were employed, with surface tensions ranging from 0.073 to 0.020 N/m, including water, ethylene glycol, ethyl alcohol and silicon fluids.

As a rule, the measurements to be taken are very simple. However, some features may interfere giving rise to erroneous results:

- (1) Depending on the type of liquid, the end of the capillary is wetted by the liquid with varying degrees of difficulty. However, it is necessary for the meniscus to be perfectly symmetrical and to reach the outer edge of the tube throughout. A second microscope was employed in our experiments to observe the entire periphery of the meniscus.
- (2) For some liquids, the surface tension  $A$  may vary widely depending on the degree of purity. Thus for ordinary ethylene glycol,  $A$  can be as low as 0.035 N/m, and it is necessary to use a very pure product for  $A$  to be equal to the generally accepted value of 0.0477 N/m. In the case of volatile liquids, the impurity content increases by evaporation, causing a variation in  $A$  with time. In the case of water, it suffices to maintain a water/vapour saturated atmosphere around the capillary tube to avoid any drop in surface tension.
- (3) The formation of microbubbles at the capillary inlet must be prevented. This can lead to significant errors in the hydrostatic pressure in the meniscus.
- (4) Capillary tube vibrations must be eliminated because they lead to maximum meniscus heights that are lower than theoretical values.
- (5) If the liquid has a very high resistivity, it is necessary to wait a sufficiently long interval between measurements to reach electrostatic equilibrium.

## 5. Results

A number of meniscus profiles were plotted from photographic enlargements. They coincided with calculated profiles within the measurement accuracy. The differences observed derived from the fact that the values of hydrostatic pressure, surface tension and radius of the capillary tube introduced into the calculations were given by the experiment, so that small errors in the actual values of these parameters may give rise to substantially different curves.

The maximum errors are always found on the axis of symmetry.

To compare a large number of theoretical and experimental results, it is necessary to select a single characteristic value of the meniscus: the height  $z_M$  on the axis of symmetry.

Figure 5 shows examples of variations in  $z_M$  as a function of potential  $U_0$  for different values of the following parameters:

- hydrostatic pressure (expressed in millimetres of liquid employed in Figs. 4–7);
- distance  $D$  from the end of the capillary tube to the plate;
- radius  $R$  of the capillary tube;
- surface tension  $A$ .

The experimental results show good agreement with theoretical results.

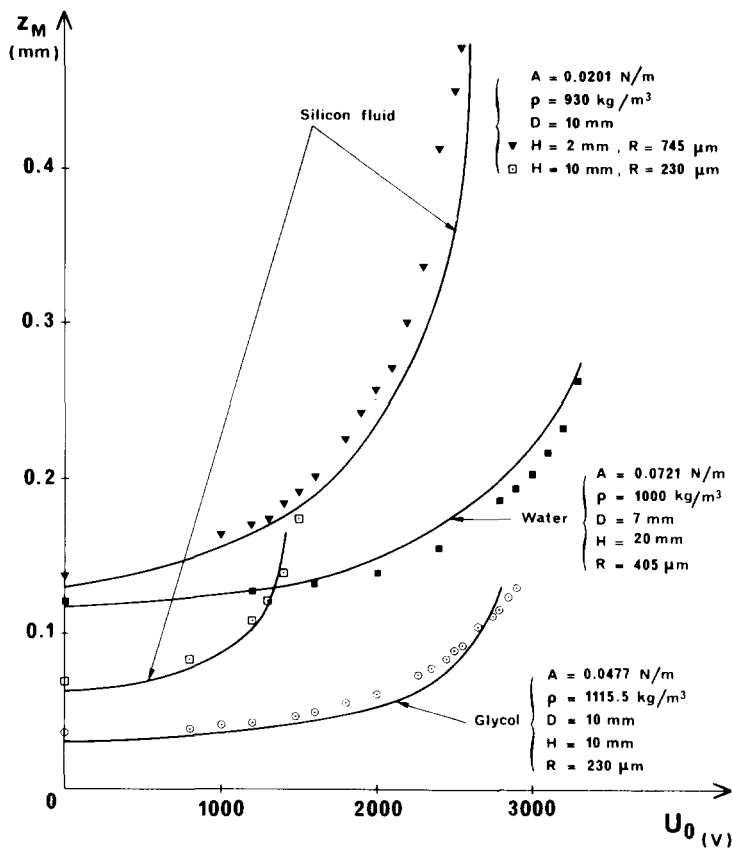


Fig. 5. Variation in height of pendent meniscus on the axis as a function of potential applied to the capillary — Comparison of theoretical curves with experimental points.

In all cases, the maximum height reached experimentally, corresponding for each measurement series to the last point reported, differed from the calculated value by less than 15/1000 mm.

The remaining experiments also confirmed the validity of the computation method developed. Hence it is possible to predict the evolution of the meniscus in accordance with various parameters. For example, for a capillary tube

directed downwards, Fig. 6 gives the heights  $z_M$  of the menisci on the axis of symmetry as a function of potential  $U_0$  and for different values of hydrostatic pressure  $p_h^0$  at the orifice. The values of the remaining parameters were:

- distance from the plate to the end of the capillary tube,  $D = 10$  mm;
- radius of capillary tube,  $R = 0.745$  mm;
- surface tension of liquid,  $A = 0.0201$  N/m.

These conditions are those of an experimental case in which the liquid was a silicon fluid with a density  $\rho$  of  $930$  kg/m<sup>3</sup>.

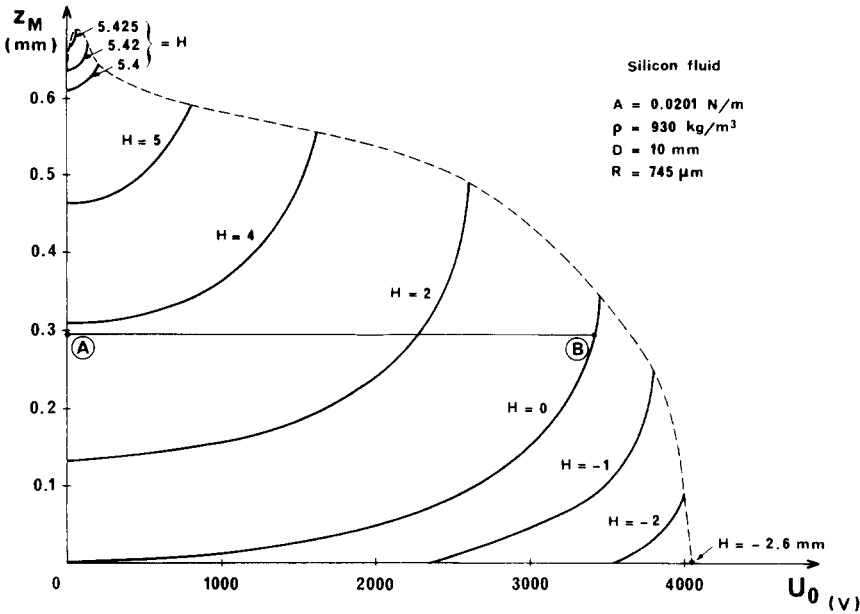


Fig. 6. Theoretical curves giving  $z_M$  as a function of  $U_0$  for different hydrostatic pressures —The dotted curve indicates the stability limit of the pendent menisci.

As a rule, a given height  $z_M$  can be reached by an infinity of combinations of the potential/hydrostatic pressure pair. Figure 7 gives theoretical profiles corresponding to points A and B in Fig. 6. The meniscus obtained by the effect of hydrostatic pressure alone is less convex than the one produced by the effect of electrostatic pressure.

For each value of pressure, a maximum potential  $U_0$  exists for which the height of the meniscus is a maximum. The dotted curve gives the boundary of the meniscus stability region. In general, if the hydrostatic pressure increases, the maximum potential decreases, but the maximum height  $z_M$  reaches greater values.

However, it is important to note two special zones located at the two ends of the dotted curve:

*Low potential zone.* At zero potential, and in the absence of gravity, the meniscus corresponding to the maximum pressure is a hemisphere, and the

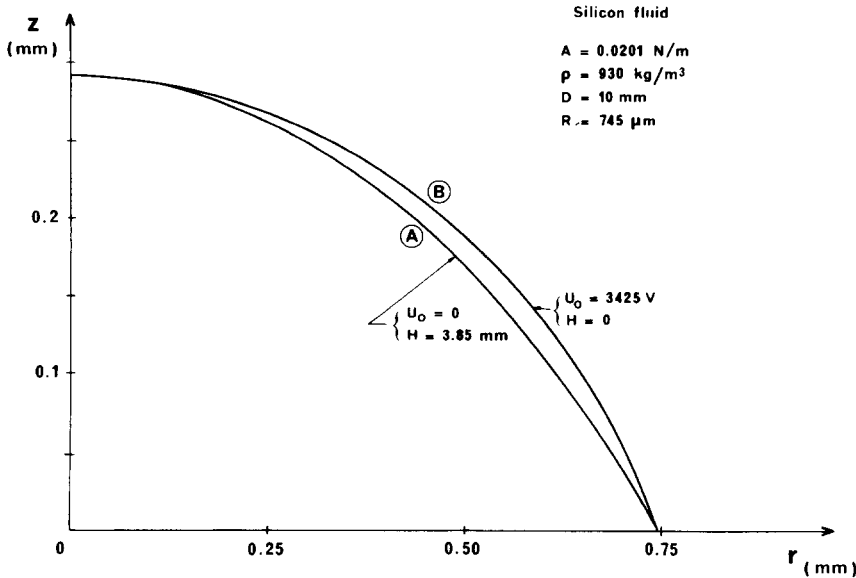


Fig. 7. Comparison of profiles of two menisci with the same height on axis, obtained respectively at zero field (A) and at zero hydrostatic pressure (B) (see Fig. 6).

maximum height  $z_M$  is equal to the radius of the capillary tube, i.e. 0.745 mm. If gravity is present (Fig. 6), this height only reaches 0.636 mm. Slightly greater heights may be obtained for non-zero potentials because the electric field has the effect of causing the meniscus profile to approach the circular shape. Note that the peak of the dotted curve can only be reached by applying a certain potential to the capillary before exceeding the maximum hydrostatic pressure at zero electric field.

*High potential zone.* If the hydrostatic pressure is negative, it is necessary to apply a strong potential to make the meniscus pass beyond the capillary outlet plane. Since the field and hence the electrostatic pressure are higher at the periphery, the meniscus displays the shape indicated in Fig. 8, of which existence is confirmed experimentally (in this case, the height on axis  $z_M$  given in Fig. 6 is not the maximum height of the meniscus).

All the results given above relate to cylindrical capillary tubes. In this case, the electric field of the meniscus surface is a maximum near the edge.

Other calculations were carried out by assigning a conical shape to the end of the capillary tube. This configuration has the effect of reducing the field on the edge of the meniscus. If the generating line of the cone is sufficiently inclined, at  $45^\circ$  for example, the maximum field is transferred to the axis of symmetry as the meniscus approaches its stability limit. However, at equivalent hydrostatic pressure, the maximum height of the meniscus is only slightly different from the value obtained with a cylindrical capillary tube of identical outlet cross-section.

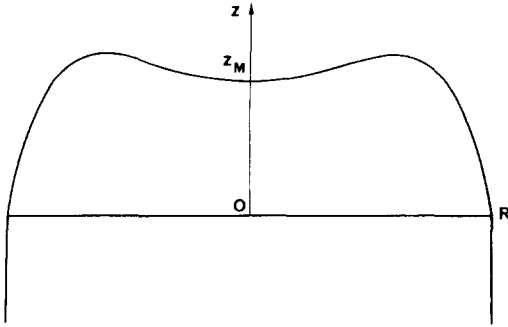


Fig. 8. Shape of a meniscus obtained with negative hydrostatic pressure and high electric potential. (The ordinate scale is much larger than the abscissa scale.)

For all the cases considered above, the zone near the tip of the meniscus remains rounded, whereas it becomes a conical shape when spraying begins. Hence to prepare the examination of conical shapes observed during the production of fine droplets, the method was adapted to the calculation of the electrostatic pressure on cones with straight generating lines. Results were obtained for the special conditions used by Taylor [9]. They clearly showed that the equilibrium of the electrostatic and capillary pressures along the generating lines can only be achieved if the hydrostatic pressure is zero and if the half-angle at the tip of the conical meniscus is equal to the value given by Taylor of  $49.3^\circ$ .

## 6. Conclusions

The computation method developed serves to predict the profile of menisci formed at the end of a vertical capillary tube raised to a certain potential in relation to a plate perpendicular to the capillary axis.

The calculations relate to stable menisci of rounded shape. For a given hydrostatic pressure they furnish the maximum potential that can be applied to maintain a stable equilibrium and the corresponding maximum height of the meniscus. The method is applicable to any liquid, irrespective of the radius of the capillary and of the distance from the plate to the end of the tube.

The theoretical results show good agreement with experimental results. It should be possible to adapt this method to solve the problem raised by conical configurations of menisci observed when the electric field is sufficiently strong to give rise to spraying of the liquid in very fine droplets.

## References

- 1 E. Borzabadi and A.G. Bailey, *J. of Electrostatics*, 5 (1978) 369.
- 2 J. Zeleny, *Phys. Rev.*, 10 (1917) 1.
- 3 B. Vonnegut and R.L. Neubauer, *J. of Colloid Sci.*, 7 (1952) 616.

- 4 C.D. Hendricks, R.F. Carson, J.J. Hogan and J.M. Schneider, *AIAA J.*, 2 (1964) 733.
- 5 A.G. Bailey and W. Balachandran, *J. of Electrostatics*, 10 (1981) 99.
- 6 D.S. Swatik and C.D. Hendricks, *AIAA J.*, 6 (1968) 1596.
- 7 J. Zeleny, *Proc. Cambridge Phil. Soc.*, 18 (1915) 71.
- 8 V.I. Kozhenkov and N.A. Fuks, *Russian Chem. Rev.*, 45 (1976) 1179.
- 9 G. Taylor, *Proc. Roy. Soc. London*, A 280 (1964) 383.
- 10 G. Taylor, *Proc. Roy. Soc. London*, A 313 (1969) 453.
- 11 F. Bashforth and J.C. Adams, *An attempt to test the theories of capillary attraction*, Cambridge Univ. Pr. G.B., 1883.
- 12 Lord Kelvin, *Popular Lectures and Addresses*, The Royal Institution, London, 1886, pt. I, p. 172.
- 13 N.L. Cross and R.G. Picknett, *Trans. Faraday. Soc.*, 59 (1963) 846.
- 14 J.F. Padday, *Surface and Colloid Science 1*. E. Matejevic and F.R. Eirich (Eds.), Wiley-Intersciences, New York, 1969.
- 15 J.F. Padday, *Phil. Trans.*, 296A (1971) 265.
- 16 A.A. Kovitz, *Proc. of the Int. Coll. on Drops and Bubbles*, California Inst. of Techn., 1974, p. 304.
- 17 M.D. Van Dyke, *Proc. Roy. Soc.*, A 313 (1969) 453. Appendix to paper by G.I. Taylor.
- 18 J.A. Becker, *The Bell Syst. Techn. J.*, (1951) 907.
- 19 J. Girerd and W. Karplus, *Traitement des Equations Différentielles*, Gauthier-Villars, Paris, 1968, p. 450.
- 20 E. Durand, *Electrostatique*, Masson, Paris, 1966, tome II, p. 59.